arXiv:0801.2484v1 [astro-ph] 16 Jan 2008

Quantifying systematic uncertainties in supernova cosmology

Jakob Nordin[1], **Ariel Goobar**[1] **and Jakob Jönsson**[1,2]

[1] Department of Physics, Stockholm University, Albanova University Center, S–106 91 Stockholm, Sweden

[2] University of Oxford Astrophysics, Denys Wilkinson Building, Keble Road, Oxford OX1 3RH, UK

Abstract. Observations of Type Ia supernovae used to map the expansion history of the Universe suffer from systematic uncertainties that need to be propagated into the estimates of cosmological parameters. We propose an iterative Monte-Carlo simulation and cosmology fitting technique (SMOCK) to investigate the impact of sources of error upon fits of the dark energy equation of state. This approach is especially useful to track the impact of non-Gaussian, correlated effects, e.g. reddening correction errors, brightness evolution of the supernovae, K-corrections, gravitational lensing, etc. While the tool is primarily aimed for studies and optimization of future instruments, we use the "Gold" data-set in Riess et al. (2007) to show examples of potential systematic uncertainties that could exceed the quoted statistical uncertainties.

E-mail: nordin@physto.se, ariel@physto.se, jacke@astro.ox.ac.uk

1. Introduction

The direct evidence for dark energy, which were obtained through observations of Type Ia supernovae (SN Ia) in the 1990s, marked the beginning of a new era in observational cosmology [1, 2, 3, 4, 5]. Significantly improved SN Ia data sets have since then been reported in e.g. [6, 7, 8, 9]. These data sets have been followed by the impressive results from the ongoing dedicated SN Ia surveys: SNLS [10] and ESSENCE [11]. An important recent compilation of published SNe Ia, including e.g. the supernovae from the first year of SNLS, but also adding several high redshift ($z \gtrsim 1$) SNe Ia from the GOODS survey, is reported in [12].

As the SN Ia sample sizes keep growing at an increased rate, the relative importance of statistical uncertainties is steadily decreasing, which brings systematic uncertainties to focus. It is thus of key importance to estimate the impact of systematic uncertainties as we enter the era of "precision cosmology".

In this work we propose a Monte Carlo simulation approach to quantify the propagated effect of known (or suspected) systematic effects in supernova cosmology. The emphasis here is to quantify the degradation of the precision to estimate cosmological parameters due to systematic errors, possibly correlated in arbitrary

groupings of supernovae: in redshift bins, by locations in the sky, observational instruments, time of observations, etc.

The current study includes investigations of sources of error from: uncertainties in the extinction by dust, K-corrections, redshift uncertainties, gravitational lensing, Malmquist bias, possible brightness evolution of the "calibrated" standard candle (e.g. metallicity effects), spectral template differences, and miss-calibrations between the low and the high redshift supernova sample. Systematic effects caused by bulk motion have been specifically targeted in a number of recent studies, e.g. [13], and were not specifically included in this study. However, some general systematic effects, e.g. drift of estimated peak brightness at low-z, would mimic the main effect expected from peculiar velocities.

The proposed method, implemented in the SMOCK package and presented in §3, allows us to quantify the sensitivity of cosmological results, obtained from real or simulated data, to specific (multiple) systematic effects. For example, we can quantify at which level a systematic effect gives rise to a bias exceeding the statistical uncertainty. The tool could hence be used to define requirements of any future mission aimed at improving our knowledge of the dark sector using SNe Ia. As an example of how this technique can be used we have performed a dedicated study of the "Gold" sample presented in Reference [12]. This study demonstrates how cosmological parameter fits are affected by a number of different systematic errors.

In §2 the model of the Universe which we have used and the cosmological parameters are introduced. Our methodology for studying the effects of systematic uncertainties is described in §3. In §4 we show how the changes in the cosmological results due to systematic uncertainties can be quantified and the trends parametrized. A number of different systematic effects, their implementation, and their effects on the Gold set are the topics of §5. Some observations regarding systematic effects and the Gold set are presented in §6. The paper is concluded by some implications for current and future SN Ia surveys in §7.

Throughout the paper units are used where the speed of light is unity, i.e. $c = 1$.

2. SN Ia magnitudes and cosmological parameters

In this paper we investigate the accuracy to which the cosmological parameters $\vec{\theta} = (\Omega_M, \Omega_X, w_0, w_a)$ can be determined. These parameters describe the matter density, Ω_M, the dark energy density, Ω_X, and the dark energy equation of state parameter, which is parametrized by $w(z) = w_0 + w_a z/(1+z)$.

The apparent magnitude in an arbitray observer filter Y, m_Y, of a SN Ia at redshift z is given by:

$$m_Y(\vec{\theta}, \mathcal{M}_X, z) = \mathcal{M}_X + 5\log_{10}\left[d'_L(\vec{\theta}, z)\right] + K_{XY}(z) + A_{XY}(z), \tag{1}$$

where

$$\mathcal{M}_X = 25 + M_X - 5\log_{10} H_0, \tag{2}$$

is a "nuisance" parameter depending on the Hubble parameter, H_0, and the brightness-shape corrected absolute magnitude, M_X, of the supernova in restframe broadband filter X. The H_0-*independent* luminosity distance is denoted by $d'_L \equiv H_0\, d_L$. K_{XY} corresponds to the K-corrections involved in the transformation between magnitudes in the restframe X-band and the observed magnitudes in the Y-band, as defined in Reference [14]. A_{XY} is a general color correction which could include, for example, corrections for host galaxy extinction in the restframe X-band (Y-band in the observer frame) and intrinsic color dispersion.

The H_0-independent luminosity distance d'_L is given by

$$d'_L = (1+z) \begin{cases} \frac{1}{\sqrt{-\Omega_K}} \sin(\sqrt{-\Omega_K}\, I) & \Omega_k < 0 \\ I & \Omega_K = 0 \\ \frac{1}{\sqrt{\Omega_K}} \sinh(\sqrt{\Omega_K}\, I) & \Omega_k > 0 \end{cases}, \tag{3}$$

$$\Omega_K = 1 - \Omega_M - \Omega_X, \tag{4}$$

$$I = \int_0^z \frac{dz'}{H'(z')}, \tag{5}$$

$$H'(z) = H(z)/H_0 = \sqrt{(1+z)^3\,\Omega_M + f(z)\,\Omega_X + (1+z)^2\,\Omega_K}, \tag{6}$$

$$f(z) = \exp\left[3\int_0^z dz'\,\frac{1+w(z')}{1+z'}\right], \tag{7}$$

where we consider, as already noted, an equation of state parametrized by

$$w(z) = w_0 + w_a z/(1+z). \tag{8}$$

We will also refer to simply 'w' when a *constant* ($w_a = 0$) equation of state parameter for dark energy is considered, e.g. in the figures showing confidence level contours in the (Ω_M, w)-plane.

In this article we focus on the implications of systematic uncertainties on the estimation of the dark energy equation of state parameter. To obtain the results presented here, a flat universe ($\Omega_K = 0$) was assumed together with constraints from the BAO peak in the SDSS sample of luminous red galaxies [15]. There the parameter

$$A = \sqrt{\Omega_m} H'(z_1)^{-1/3} \left[\frac{1}{z_1}\int_0^{z_1} \frac{dz'}{H'(z')}\right]^{2/3} \tag{9}$$

was measured to great precision at $z_1 = 0.35$: $A = 0.469 \pm 0.017$. This was included as a prior.

Moreover, when showing results for the (w_0, w_a)-plane we marginalize over the Ω_M parameter. The method, presented in the next section, can of course be applied to any other cosmological parameters using any combination of priors.

3. Methodology

The aim of this study is to investigate how different systematic effects influence the cosmological parameters obtained from fits on a set of SNe Ia. In order to take both

statistic errors and systematic effects into account, we use Monte Carlo simulations. The method, in short, consists of the following steps:

(i) The original data-set, consisting (minimally) of supernova redshifts and peak magnitudes, is used as a starting point‡. Other properties, like excess color, can be included as well. A perturbed synthetic data-set is generated by randomizing these quantities for each supernova according to either measurement uncertainties and/or assumed dispersion in the original data-set and the systematic effect(s). This is done taking into account possible correlations between supernovae.

(ii) Cosmological parameters, $\vec{\theta}$, are fitted to the perturbed data-set.

(iii) The first two steps are repeated many times and the density of best fit values of cosmological parameters are used to trace out confidence level contours. From the relative location and shape of these contours it is possible to understand and to quantify the influence of systematic effects, both in terms of potential biases and enlarged confidence level contours.

Let us now elaborate on and motivate these steps.

The original data-set in step (i) could either be a simulated data-set, corresponding to a known cosmology, or a real data-set for which we would like to study the expected effects of systematic errors.

When the perturbed synthetic data-sets are generated, all applicable uncertainties and biases are used to compute the supernova redshifts and peak magnitudes. Since many sources of error may be included in a single run, each contribution is co-added in the final perturbed synthetic supernova data. For example, the distance modulus to a simulated supernova can be computed in several steps, each adding a modification to the apparent magnitude. First, statistical uncertainties are taken into account: a value of the peak magnitude (e.g. in rest-frame B-band) is drawn from a Gaussian distribution centered around the original supernova brightness and with standard deviation corresponding to the intrinsic brightness scatter together with (for real data) the measurement error added in quadrature. Thereafter, other perturbations are added. For example, a constant bias, mimicking a calibration error, could be added to all SNe Ia in a particular redshift bin.

Color errors or spectral template changes, and the related reddening corrections, also result in offsets from the originally derived distance modulus. Redshift uncertainties are generated from the probability distribution, if given by photometric redshift error studies, or by a smaller Gaussian error, if spectroscopic. All of the above modifications can be applied to the complete data set or just a subset (e.g. only high redshift objects). If only the intrinsic scatter, the measurement error or the sum added in quadrature is used (and assumed to be Gaussian in magnitudes), the standard analysis of the data-set is retrieved.

‡ Instead of these derived properties, the supernovae could be described by their light curves observed in different wavelength bands. So far, our code does not calculate errors from modifications of individual measurement points.

In this paper, such a data-set will be referred to as a "clean" data-set. Two advantages with this method are that uncertainties and biases can be *non-Gaussian* and *correlated*.

Non-Gaussian error distributions can be studied since the measurements can be randomized according to any arbitrary distribution. Examples of such distributions are the dimming by dust and gravitational lensing magnification. Arbitrary correlations can be created through modifications of subsets of the data.

Any uncertainties in priors used should also be incorporated according to this method. If the prior is Gaussian, a value of the prior is drawn from a Gaussian distribution for each iteration.

In step (ii) the best fit cosmological parameters $\vec{\theta}$ for the synthetic data-set are found using a maximum likelihood technique.

In this paper, a likelihood analysis taking only Gaussian errors into account is performed. To find the best fit cosmological parameters to the synthetic data-set, the negative likelihood is minimized using the Powell algorithm [16] implemented in the SNALYS fitting routine within the SNOC package [17].

In step (iii) we use the best fit values of $\vec{\theta}$ from a large number of realizations of synthetic data-sets to construct confidence level contours. The best fit parameters $\vec{\theta}$ obtained for each synthetic data-set can hence be viewed upon as one possible "measurement" of the cosmological parameters including systematic uncertainties. The ensemble of best-fit values stemming from the iteration procedure maps out the confidence region of possible "measurements" given the data with systematic and statistical uncertainties. Figure 1 shows examples of the best fit values of w and Ω_M as well as w_0 and w_a for 8000 perturbed "Gold" data-sets. In each case, the fit also includes a BAO prior from [15]. To obtain the confidence level contours in Figure 1 and subsequent figures we use the density of best fit values of the cosmological parameters $\vec{\theta}$. The contours corresponding to e.g. the 68.3% confidence level in the plane spanned by Ω_M and w (right panel in Figure 1) and w_0 and w_a (left panel) are found by identifying the isocontours which enclose 68.3% of the points.§ We have checked that the confidence level contours obtained in this way agrees with contours from standard χ^2 minimization, when the errors are Gaussian and uncorrelated. In the standard interpretation of confidence level contours, the 68.3% confidence level contour, for example, is the contour which fulfills $\chi^2 = \chi^2_{\rm min} + 2.30$. ‖

This iterative method was developed mainly in order to take correlated and non-Gaussian errors into account (e.g. from extinction and gravitational lensing). When using standard maximum likelihood techniques, all errors are required to be Gaussian and the correlation matrix has to be calculated and inverted for each systematic error.

§ For figures displayed here we have used the elliptic contour that closest match the true isocontour. The two are generally similar and elliptic contours make comparisons clearer.

‖ Subtle differences between the two interpretations of confidence level could arrise. So far no deviations have been detected, but a more dedicated study might be of interest and is a possible topic for future SMOCK-related work.

When dealing with large data-sets this inversion can be numerically cumbersum and extremelly time-consuming. Using the SMOCK method this is avoided - each iteration is treated as a single occurrence and only the best fit is calculated.¶ It should be noted that in this fit [step (ii)] we use the standard procedure of assuming all SNe Ia to be uncorrelated with Gaussian errors, but since a) only the best fit is calculated and b) a large number of individual fits are used the result will be more accurate and the process less demanding for large data-sets.

The code developed to run the loop consisting of steps (i)-(iii), and in particular to generate simulated data-sets taking systematic effects into account in a flexible way, is collected in the SMOCK package.

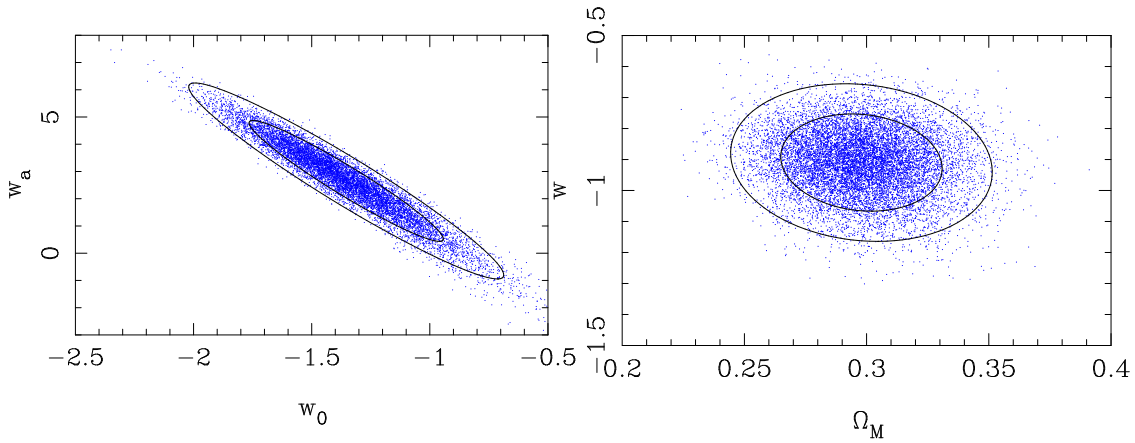


Figure 1. Examples of the outcome of a SMOCK run. The points show the best fit values of 8000 simulated data sets similar to the Gold data set. The inner and outer contours, obtained from the density of points, correspond to 68.3% and 95.4% confidence level. Left and right panels show the best fit values in the (w_0, w_a)-plane and (Ω_M, w)-plane, respectively.

3.1. An example: the Gold data-set

As a test case, we have chosen to study the "Gold" sample presented in Reference [12]$^+$. The data-set was further divided into three primary redshift bins: i) 36 low-z SNe Ia ($z < 0.1$), ii) 90 intermediate redshift SNe Ia ($0.1 < z < 0.7$), and iii) 56 high-z SNe Ia ($z > 0.7$). This division in redshift space was done in order to study the impact from systematic effects applied at different redshifts. It should be emphasized that this division of supernovae is somewhat arbitrary and mostly done for demonstration purposes. However, the redshift bins broadly correspond to i) the near-by SN Ia sample used to anchor the Hubble diagram [18, 19, 20], ii) the ground based data from the

¶ The covariance matrix for any error could in principle be calculated through the Monte Carlo simulated data-sets.

$^+$ From which we have used SN Ia redshifts, colors, magnitudes and corresponding errors. The colors were derived from the host galaxy extinction, A_V, through the assumption of $E(B-V) = A_V/R_V$ where $R_V = 3.1$.

High-Z Team, the Supernova Cosmology Project and the SNLS, and iii) the HST data from the highest-z SNe Ia.

4. Propagation of systematic effects

Through repeated SMOCK runs using a range of errors of different magnitudes we are able to make comparisons between the impact on fitted cosmological parameters from different systematic effects and standard statistical uncertainties. Figure 2 shows an example of the parameter fits which would result if the peak brightness magnitudes of the high-z sample were positively biased. The solid contour shows the 68.3% confidence level contour for the unperturbed (clean) sample, which only suffers from statistical uncertainties. The other contours in the figure correspond to data sets affected by high redshift apparent magnitude bias in the range 0.01 to 0.15 mag. An archive consisting of figures of *all* systematic effects individually applied to each redshift bin in the Gold set can be found at the SMOCK webpage www.physto.se/~nordin/smock.

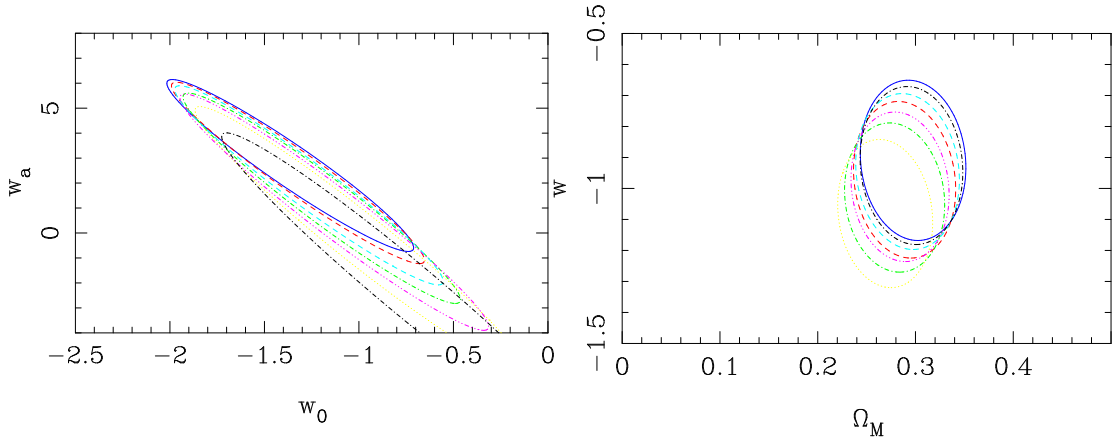


Figure 2. Effect on cosmological results due to high-z SN Ia with biased magnitudes. Left and right panels show 68.3% confidence level contours in the (w_0, w_a)-plane and (Ω_M, w)-plane, respectively. Solid (blue) contours correspond to the results of the clean run, which only take into account statistical uncertainties. The other contours show the effect of adding bias of 0.01, 0.03, 0.05, 0.07, 0.1, and 0.15 mag. Flat universe and BAO prior assumed.

To further quantify and compare different systematics we have monitored the functional dependence of the fitted parameters $\vec{\theta}$ and some other indicators on the assumed systematics. In what follows we will refer to the shift of the best fitted values or its changing uncertainty due to increased systematic effects as the "evolution" of a parameter or indicator. In particular, we will exemplify the evolution of five parameters and indicators due to increasing levels of systematic uncertainties:

(i) The evolution of (best fit) Ω_M and w.

(ii) The evolution of (best fit) w_0 and w_a.

(iii) The evolution of the size (area) of the confidence level contours*.

(iv) The evolution of the *total area*. This is defined as the complete confidence region that would have to be used *if* the systematic error was suspected.♯

(v) The increased dispersion around the best fit model in the Hubble diagram. Possible systematic effects that increase the scatter above some limit would be considered unrealistic.

We have parametrized the evolution of the five parameters and indicators listed above as a function of the magnitude of the systematic effects. The goodness of each parameterization is estimated through the residual scatter around the best fit of the evolution. Notice that these parameterizations depend on the data set used and the redshift binning chosen. In most cases a parameterization linear with the size of the systematic effect yields a good fit. Where quadratic or exponential parameterizations have been used, this is noted.

Uncertainties added to the SN Ia data affect the dispersion in the Hubble diagram. This provides a way of estimating whether systematic effects are realistic or not - a systematic effect introducing a dispersion larger than the observed one is unlikely. We have therefore also monitored the added *dispersion* on the Hubble diagram as systematic effects were introduced (i.e. increased residual scatter around the best fit cosmology). We find that constant bias often yield very small changes in the original dispersion, while added scatter give rise to increased dispersion, as expected. In general, the bias from systematic effects begin to dominate over statistical errors well before causing a noticeable increase in the residuals in the Hubble diagram. A typical example will be discussed below (see §5.4).

As an example of how the SMOCK technique could be used, we calculate the limits for when each individual systematic effect will dominate over the statistical errors for the Gold data-set. This was defined to occur either when the area of the 95.4% confidence level contour in the (Ω_M, w)-plane or the (w_0, w_a)-plane was doubled (compared to the clean fit) or when the best fit of Ω_M or w or, in the other case, w_0 or w_a was outside the 95.4% confidence level region of the clean fit. This might be called the point of "systematic-statistic equality", and is used by us to compare the relative importance of different systematic effects. These points are summarized in Table 1 (for the $w_0 - w_a$ parametrization) and Table 2 (for the $\Omega_M - w$ parametrization).

Figure 3 shows the evolution of the parameters and indicators described in Section 4 for the Gold sample with added constant magnitude bias. Figure 4 shows the evolution in the (Ω_M, w) plane when the absolute magnitude of SN Ia evolves with redshift. Graphs showing the evolution of systematic errors for a larger range of simulated errors can

* This area is always used in comparison to the area corresponding to the clean sample.

♯ This parameter will depend on the changes of the first three, as well as the relative "direction" of error propagation in the fitted parameter plane. Looking at Figure 2, an uncertainty of up to 0.15 mag would mean that the *total* area covered by *any* ellipse plotted should be included in the total area. This area is quoted compared to the area corresponding to the clean sample.

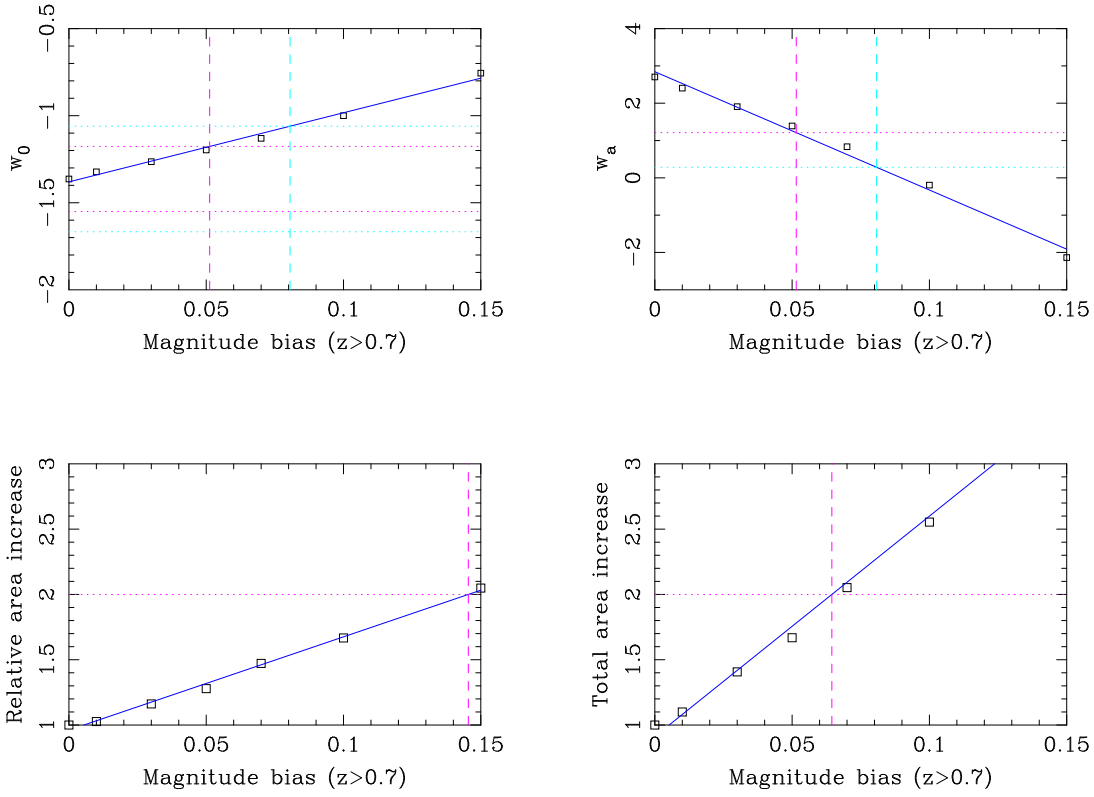


Figure 3. Magnitude bias for high-z SN Ia (systematic offset for all SNe with $z > 0.7$). Horizontal lines in the top left and top right plot show the limits when the statistical 68.3% and 95.4% confidence levels are reached by systematics. In the bottom left and bottom right plot the horizontal lines show when the area relative to the clean run is doubled. Vertical lines show at which error (if so) these limits are reached. This signifies either a bias creating an effect larger than the statistical uncertainty or a systematic uncertainty doubling the size of the regions (or a combination thereof).

be found at www.physto.se/˜nordin/smock. Some of the main results for the different systematics are presented below.

5. Specific sources of systematic errors

In the current study, we have concentrated on a limited number of tests for systematic effects. We emphasize that the SMOCK code is flexible enough to easily incorporate further effects. In this section we discuss motivations, implementations and general results of the systematic effects we have studied.

The color correction A_{XY} was modelled according to the Galactic extinction law in Reference [21], with the parameter $R_V = A_V/E(B-V)$ specifing the wavelength dependence. If an average Milky Way value of $R_V = 3.1$ is assumed, it is possible to determine A_V (i.e. restframe V-band absorption) through the measured supernova color excess, $E(B-V)$. In studying systematic effects we are not concerned with the absolute value of the correction A_{XY}, but in its change as any of the parameters R_V

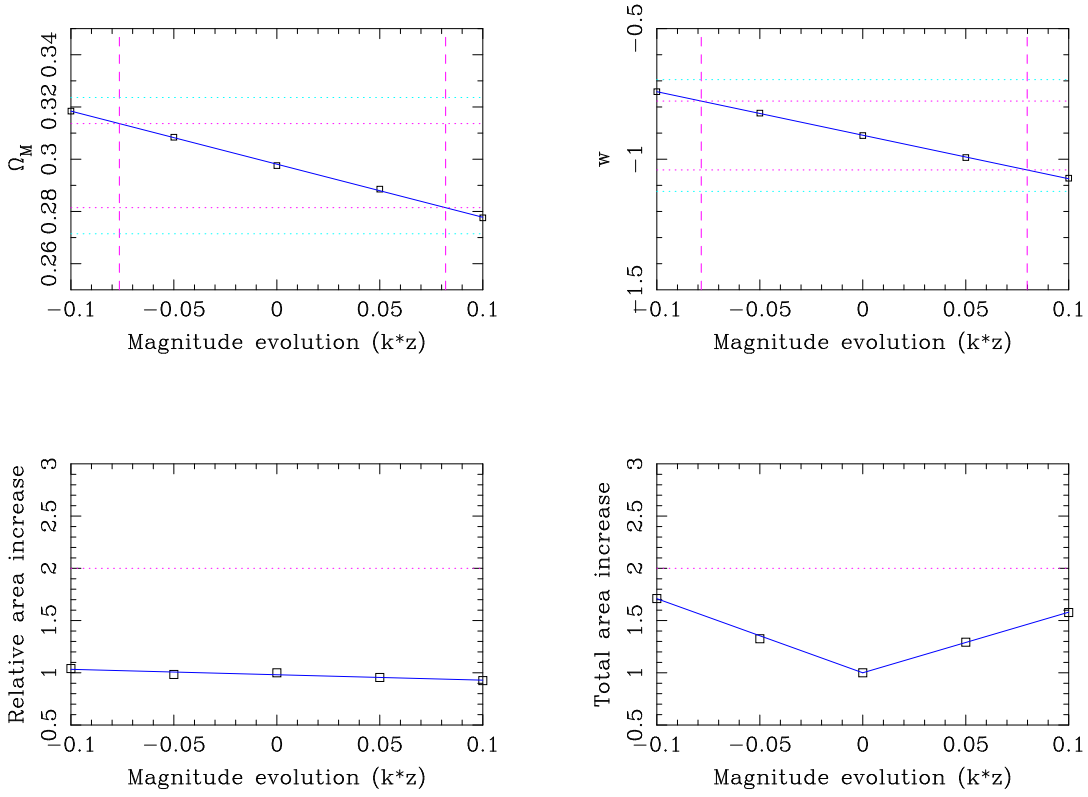


Figure 4. Bias in the $(\Omega_M,)w$-plane caused by evolution of peak brightness as a function of redshift. Horizontal lines in the two top plots show limits when statistical 68.3% and 95.4% confidence levels are reached by systematics. In area plots horizontal lines show when the area relative to the clean run is doubled. Vertical lines show at which error (if so) these limits are reached. This signifies either an introduced bias creating an effect larger than the statistical uncertainty or an introduced uncertainty doubling the size of the regions (or a combination thereof).

and $E(B-V)$ change.

A particular difficulty comes with the use of cross filter K-corrections, $K_{XY}(z)$, and spectral templates. Applying accurate K-corrections is notoriously challenging since they rely on spectral templates from compilations of nearby supernovae. Obtaining a spectral sequence as a function of time for each high redshift SN Ia is practically impossible with current allocation of instruments for follow-up observations. Since the same spectral templates are often used, any errors in the templates would propagate through the K-corrections and give rise to correlated errors between supernovae at similar redshifts.

We have included the effects of possible systematic effects due to K-corrections and color corrections in two ways:

(i) When any of the parameters (e.g. z, $E(B-V)$ or R_V), were perturbed both clean and perturbed corrections were calculated for each SN Ia†† and the difference was

†† These perturbed corrections include integration of the filter with extincted and redshifted spectra.

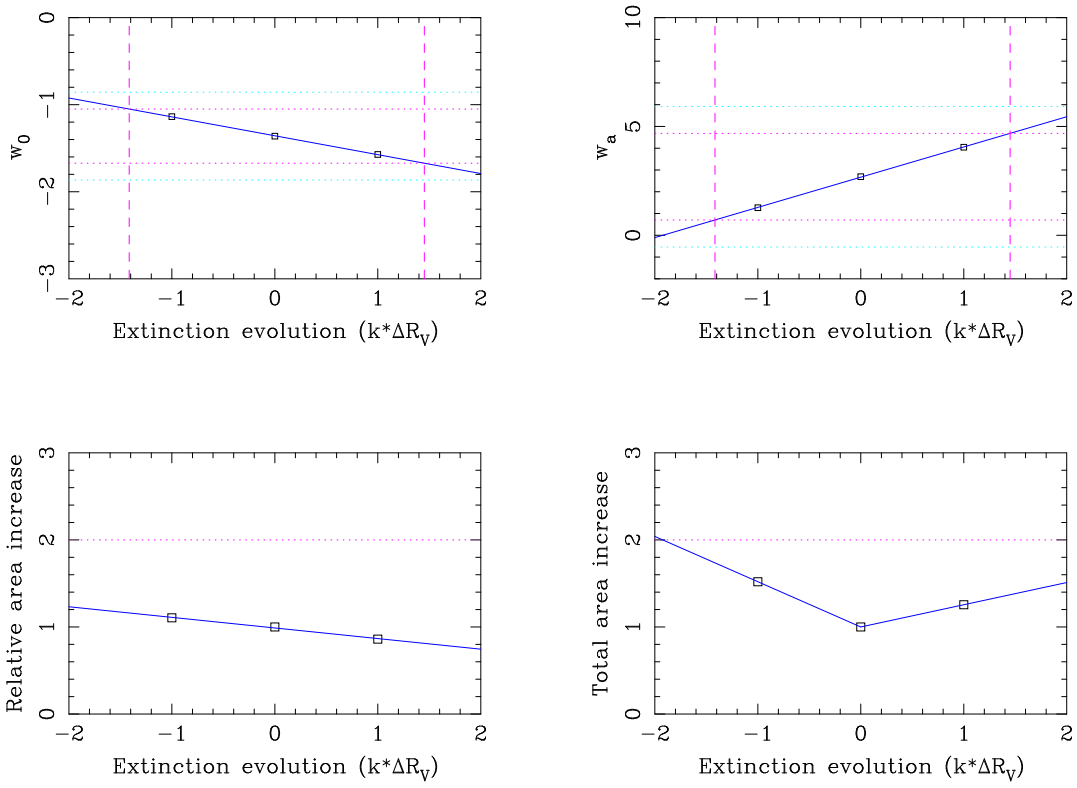


Figure 5. Effects from dust extinction evolving with redshift parameterized as a linear modification ($\delta R_v = k * z$, k systematic error) of local (Milky Way) values. Effects on $w_0 - w_a$ plane demonstrated. Horizontal lines in the two top plots show limits when statistical 68.3% and 95.4% confidence levels are reached by systematics. In area plots horizontal lines show when the area relative to the clean run is doubled. Vertical lines show at which error (if so) these limits are reached. This signifies either an introduced bias creating an effect larger than the statistical uncertainty or an introduced uncertainty doubling the size of the regions (or a combination thereof).

used as an individual SN Ia magnitude modification.

(ii) To study the effects from different spectral templates we compared the differences in cosmological results which occur for three different spectral templates used in the calculation of the K-corrections.

In order to study variations with redshift, systematic effects were applied to individual redshift bins. It is important to notice that systematic errors, including K-corrections, usually do not add linearly. For realistic combinations of different errors, simulations combining all of these are necessary. A simple addition of errors due to different systematic effects might consequently not correspond to the true combined error.

We have used standard Bessel filters for this study and unless otherwise specified a modified Nugent-type spectral template [28]. In each individual K-correction calculation, the filter most overlapping with the B-filter redshifted by a factor $(1 + z)$ is used.

Table 1. Points of systematic-statistic equality for different systematics. Parameters and indicators in the table are described in Section 4. All fits are linear unless otherwise noted.

Error	z-bin	w_0	w_a	Area	Tot. Area
$E(B-V)$ bias	high	0.011	0.011	—	0.015
$E(B-V)$ bias	int	0.016	0.016	—	0.031
$E(B-V)$ bias	low	0.015	0.014	—	0.022
$E(B-V)$ spread	high	—	—	0.086[a]	0.084[a]
$E(B-V)$ spread	int	—	—	0.031	0.031
$E(B-V)$ spread	low	—	—	0.100	0.098
Evolution	all	0.09	0.09	0.5	0.1
Mag bias	high	0.051	0.051	0.145	0.064
Mag bias	int	0.064	0.064	−0.742	0.128
Mag bias	low	0.058	0.057	1.353	0.098
Mag spread	high	2.582	2.607	0.398[a]	0.389[a]
Mag spread	int	2.798	2.731	0.287[b]	0.279[b]
Mag spread	low	—	—	0.412[b]	0.408[b]
Lensing	all	—	—	4.9% inc.	—
R_V spread	all	18.433	18.586	1.132[b]	1.109[b]
R_V spread	high	42.159	48.616	13.399	13.168
R_V spread	int	5.548	3.610	−11.903	−58.987
R_V spread	low	2.006	1.950	−0.882	−1.454
R_V bias	high	1.7	1.7	—	—
R_V bias	int	11.0	11.0	—	—
R_V bias	low	1.1	1.1	—	—
R_V bias	all	0.4	0.4	—	—
Redshift bias	high	0.045	0.040	−0.171	0.108
Redshift bias	int	0.007	0.007	0.012	0.006
Redshift bias	low	0.001	0.001	−0.028	0.002
Photometric z	all	0.006[b]	0.006[b]	0.003[a]	0.003[a]
Redshift spread	high	0.141	0.140	0.597	0.166
Redshift spread	int	0.068[b]	0.051[b]	0.042[b]	0.035[b]
Redshift spread	low	0.008[b]	0.008[b]	0.004[b]	0.003[b]
R_V Evolution	all	1.452	1.450	—	—
Malmquist bias	high	11.4%	11.4%	—	—
Malmquist bias	int	26.9%	28.0%	—	—
Malmquist bias	low	71.2%	75.7%	—	50%

[a] An exponential fit to the error level had to be used to reach good precision
[b] A quadratic fit to the error level had to be used to reach good precision.

5.1. Magnitude bias or dispersion

Instrumentation errors, calibration errors, peculiar velocities, or bulk motion could in principle give rise to redshift dependent bias or increased dispersion in SN Ia magnitudes. We have investigated the effects of magnitude bias and dispersion for different redshifts. Figure 2 shows an example of the effect of magnitude bias for the high redshift bin.

Table 2. Points of systematic-statistic equality for different systematics. Parameters and indicators in the table are described in Section 4. All fits are linear unless otherwise noted.

Error	z-bin	Ω_M	w	Area	Tot. Area
Bias	high	0.103	0.100	—	0.277
Bias	int	0.181	0.179	—	0.198
Bias	low	0.070	0.069	—	0.128
$E(B-V)$ bias	high	0.024	0.024	—	0.067
$E(B-V)$ bias	int	0.036	0.037	—	0.040
$E(B-V)$ bias	low	0.017	0.017	—	0.033
$E(B-V)$ spread	high	—	—	0.222	0.214
$E(B-V)$ spread	int	—	—	0.380	0.378
$E(B-V)$ spread	low	—	—	0.126	0.122
Mag evolution	all	0.081	0.080	—	0.326
Malmquist bias	high	24.8%	25.6%	—	—
Malmquist bias	int	50.9%	49.7%	—	—
Malmquist bias	low	65.7%	66.2%	—	69.4%
R_V bias	high	4.0	4.0	—	—
R_V bias	int	14.2	12.8	—	—
R_V bias	low	1.2	1.2	—	—
R_V evolution	all	3.964	3.932	—	—
R_V spread	all	—	—	3.717	3.482
R_V spread	high	—	—	10.650	11.482
R_V spread	int	—	—	35.443	36.061
R_V spread	low	—	—	7.445	7.172
Mag spread	high	0.961	0.948	2.869	1.162
Mag spread	int	2.805	2.511	10.656	3.012
Mag spread	low	0.698	0.721	0.803	0.508
Redshift bias	high	0.039	0.039	—	—
Redshift bias	int	0.085	0.092	—	—
Redshift bias	low	0.001	0.001	—	—
Photometric z	all	0.007	0.007	0.007	0.005
Redshift spread	high	0.644	0.693	0.396	0.296
Redshift spread	int	0.032	0.032	0.271	0.042
Redshift spread	low	0.007	0.007	0.008	0.005

Results An additional Gaussian dispersion (e.g. due to measurement errors and intrinsic dispersion) give rise to increased confidence level contours and do not introduce any bias, as expected. Constant magnitude bias, on the other hand, induces a roughly linear bias in the cosmological parameter fits. Qualitative confirmation of this can be found from the points of systematic-statistic equality as given in Table 1. An increased magnitude dispersion does not cause any systematic shift in w_0 or w_a. However, a dispersion of 0.40, 0.29 or 0.41 magnitudes added to the low, intermediate, or high redshift bin, respectively, doubles the size of the confidence regions. In a similar way a constant magnitude bias of roughly $\Delta M = 0.05$ (slightly depending on redshift range) shifts the position of the 95.4% confidence level contour so that the best fit corresponding

to unbiased data lies outside the contour.

The direction of the resulting bias in the (w_0, w_a)-plane depends on the redshift of the biased supernovae. A constant magnitude bias in the intermediate-z bin gives rise to a bias roughly along the major axis of the confidence level contour in the (w_0, w_a)-plane. A magnitude bias affecting only the high-z bin, on the other hand, induces a shift roughly along the direction perpendicular to the intermediate-z case, i.e. along the semi-major axis of the confidence level contour. The cosmological results are consequently more sensitive to a constant magnitude bias at high-z† than at intermediate-z.

Similar trends can be seen in the (Ω_M, w)-plane, although the fits are roughly twice as stable considering systematic magnitude modifications (a bias of rougly $\Delta M = 0.1$ mag would reach statistical-systematic equality).

Notice that these runs do not include the effects on color determination that magnitude errors could create (see §5.3 on color effects below).

5.2. Redshift uncertainties

The uncertainty in redshift propagates mainly in four ways into the estimation of cosmological parameters:

(i) The lightcurve shape parameter used in the width-brightness relation, e.g. the "stretch" factor s (see [22]) is degenerate with the redshift as the latter is obtained from a fit of $s(1+z)$ to the light curve. An error in $(1+z)$ is thus compensated by a corresponding error in s.

(ii) The K-corrections applied correspond to the wrong redshift.

(iii) The estimate of the color excess is biased.

(iv) The points are offset in the horizontal axis of the Hubble diagram.

Points (i) and (iv) can be studied either separately or together, results quoted here include effects (ii-iv) combined: no specific light curve shape dependent modifications were included in the current version of the code, but this is a simple extension planned for future studies since $\delta z = \delta s$.

Results As long as spectroscopic redshifts are available either from the host galaxy or the SN Ia, the redshift uncertainty would typically only affect the second or third decimal place of the measured redshift. This is the case for most if not all the SNe Ia in the Gold sample. We note that a bias in the redshifts of the low-z (int-z) bin at the level of $\Delta z = 0.001$ ($\Delta z = 0.007$) would suffice to exceed the statitsical uncertainty (when considering the $w_0 - w_a$ paramerization). Thus, this source of error is not negligible, although it is unlikely to be a major concern. However, future large-scale surveys may have to rely upon photometric redshifts for a large fraction of the supernovae. Studies

† It might be of interest to note that adding a high-z bias of $\Delta M = 0.1$ mag brings the best fit of the Gold data-set from a slight "offset" to quite precisely that corresponding to a cosmological constant, $(w_0, w_a) = (-1, 0)$.

of photometric redshifts [23, 24, 25] have shown that the uncertainties are proportional to $(1 + z)$. We model the size of the photometric redshift errors using the formula $\delta z = k(1 + z)$, where the size of the uncertainty is described by the parameter k. We have studied the increased uncertainty due to this fact, when applied to all supernovae, for several different values of k. Photometric redshift uncertainties can give rise to large effects. Notable is that Gaussian uncertainties can give rise to significant bias. For the whole sample, the point of systematic-statistic equality is reached when the photometric redshift error is $\delta z = 0.006(1 + z)$ (see Table 1). Since d'_L changes rather slowly at high redshift, we expect the cosmological results to be more sensitive to redshift uncertainties at low and intermediate redshift than at high redshift. This is in agreement with what we find. If only the low redshift bin is affected by photometric redshift errors, the systematic errors starts to dominate at $k = 0.008$. Since this value of k is only slightly larger than what is needed for the whole sample, we conclude that spectroscopic redshifts are particularly important for low redshift SNe Ia. The same general trend can be seen in the $\Omega_M - w$ parameterization.

5.3. Systematic effects on color

Any bias or error in measurements of apparent magnitudes will propagate to the color determination and hence affect corrections for extinction. Biased magnitudes due to miscalibration between different filters could hence result in color errors. Use of multi-band color estimations would help stabilizing color systematics, to some extent limiting these effects. Both constant offsets and Gaussian errors in the color excess, $E(B - V)$, were considered as systematic effects.

Results Estimation of cosmological parameters is very sensitive to errors in colors: Already a bias of 0.02 in $E(B - V)$ applied to any of the redshift bins would create a significant bias in the (w_0, w_a)-plane. For a significant bias in the (Ω_M, w)-plane, a bias of 0.03 is sufficient. Since $E(B - V)$ is a differential calculated from two (or more) filters this shows the extreme care necessary in photometry and filter calibration. The intrinsic colors of SNe Ia are poorly known, especially at high redshift. Thus, we rank this source of error as a critical one.

5.4. R_V systematic effects

R_V values, being the reddening due to interstellar dust in the host galaxy or a combination of effects including SN Ia physics and/or circumstellar dust, are notoriously hard to determine. We have studied how much offsets or random fluctuations from a fixed Milky Way-like value of $R_V = 3.1$ affect confidence level contours. The results indicate the systematic effects which arise from using $R_V = 3.1$ in the calculations while the *true* value is different. If the average value deviates significantly from current Milky Way estimates, a systematic bias will occur in any cosmology fit.

In this case, the systematic effect was introduced for all SNe Ia (allowing for the fact that virtually no host galaxy R_V's are known) as well as to the members of each bin separately.

As an example of how systematic effects influence the scatter in the Hubble diagram, consider a bias in R_V for high-z SN Ia. The rms dispersion around the best fit Hubble diagram for different R_V values is shown in the left panel in Figure 6. The right panel in Figure 6 shows the dispersion in the Hubble diagram for different values of the dispersion, σ_{R_V}, in R_V. From the figure we conclude that there is no dramatic increase in the Hubble diagram dispersion for the range of R_V and σ_{R_V} considered.‡ Other systematics yield similar results.

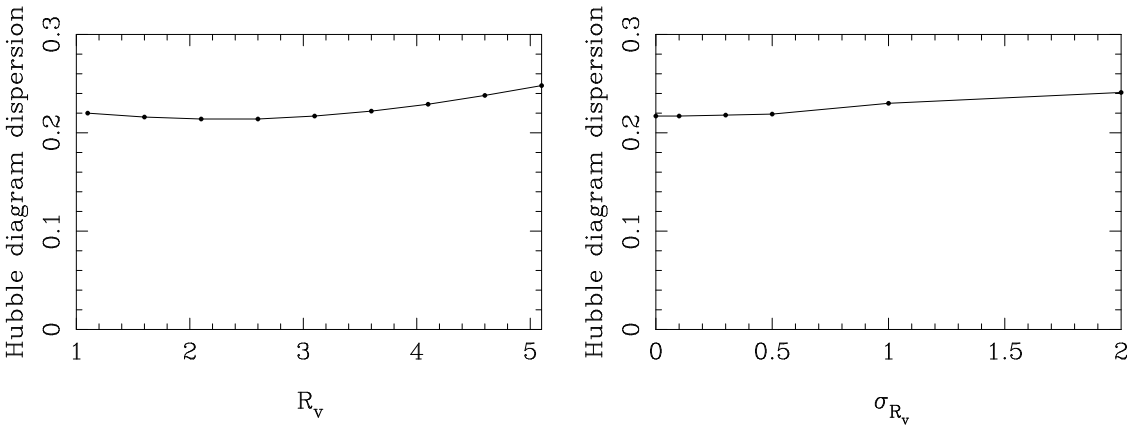


Figure 6. Dispersion (rms) in the Hubble diagram due to uncertainties in R_V for high redshift SNe Ia. The right panel shows how the dispersion changes for different values of R_V. The left panel shows the effect of increasing the Gaussian dispersion in R_V.

Results As can be seen from Table 1 a Gaussian with fairly large width ($\sigma_{R_V} = 1.13$) can be added to all SNe Ia before reaching the current statistical limit even for $w_0 - w_a$ fits.

But this assumes an R_V distribution which is *both* centered on 3.1 and Gaussian. A non-Gaussian distribution could for example arise from different dust properties in different galaxy types. Simulations of systematic effects due to non-Gaussian distributions is another possible future application of SMOCK. An offset in the assumed value of total to selective extinction coefficient of $\Delta R_V = 2$ would be required to significantely bias the results. We note that this is at the level of discrepancy between the Galactic value and what has been derived from SNe Ia with the SALT technique [29, 30]. A linear evolution in redshift $dR_V/dz \approx 1.5$ (R_V evolution in Table 1) would be required to exceed the statistical uncertainty in the Gold data-set.

‡ A close inspection of Figure 6 reveals a *slightly smaller* dispersion if a small negative R_v bias is added. This shows that care is needed when minimizing hubble diagram residuals since a systematic bias can be introduced.

The importance of SN Ia colors can be seen here: For the intermediate redshift bin, the current data-set have average colors close to zero making this redshift bin less sensitive to R_V-bias. This shows the advantage of low extinction supernovae and in general the promise of how future subsets of SNe Ia could be used to limit systematics. Obviously, actual knowledge of host galaxy dust properties would be preferable.

5.5. Malmquist bias

An effect corresponding to Malmquist bias, the systematic failure to detect the faintest elements of a population, was implemented through the option to, in a specific redshift interval, remove a certain fraction of the faintest SNe Ia and replace them with a (for one SMOCK iteration only) random copy of the *same number* of other SN Ia in the same redshift interval.§

Results Adding a synthetic Malmquist bias is more natural for a completely simulated data-set, but runs using the Gold-set does give some indication of the size of the effect.

Results were quite stable to Malmquist bias added to the data in the low and intermediate redshift bins. A significant bias did arise when Malmquist bias was added to the high-z bin, but in order for the effect to dominate over the statistical uncertainty a Malmquist ratio (the fraction of elements removed) of about 11% is required. This would need to be a systematic effect affecting all SNe Ia above $z = 0.7$. In the (Ω_M, w)-plane the 25% faintest SNe Ia would have to be missed by a survey to reach the statistical error limit.

5.6. Gravitational lensing

Gravitational lensing due to matter along the line of sight to a supernova, could give rise to amplification or de-amplification of the observed flux. The effect of gravitational lensing can be described by the magnification factor μ. Due to flux conservation the average flux from a large number of standard candles is the same as the flux from a standard candle not affected by lensing. The average magnification factor is consequently $\langle\mu\rangle = 1$. A standard candle brighter or fainter than average would be described by $\mu > 1$ and $\mu < 1$, respectively. Gravitational lensing increases the dispersion of standard candles and could give rise to a selection bias, since amplified SN Ia are easier to detect than de-amplified ones. The more distant the standard candle, the more likely it is to be affected by gravitational lensing since the light emitted from it traverses more matter. When gravitational lensing is included, all SN Ia magnitudes are modified by a term $-2.5\log_{10}\mu$, where the magnification factors are drawn from appropriate redshift dependent probability distribution functions generated using the SNOC package [17].

§ For a real data-set it might be more relevent to apply a "reversed" Malmquist effect, by removing a *negative* fraction of dim SNe Ia. This will with the current SMOCK-code add new dim objects.

Results Added lensing uncertainties does not significantly change the cosmological results, in accordance with earlier estimates [26]. This is an example of how detailed studies of possible systematics can lead to a situation where a systematic uncertainty can be said to be under control.

5.7. SN Ia spectral templates

We have compared the results obtained using different spectral templates when calculating the K-corrections. The data were refitted using both our standard modified Nugent template [27, 28] and two other publicly available templates [30, 31]. This refitting procedure includes new extinction estimates and new K-correction calculations. The effects of different templates were studied using two modes: (i) Either the deviation of magnitude at epoch 0 (the date of maximum B-band brightness) due to template differences from our standard template was used or (ii) the *maximal* deviation at either epoch -10, 0 or $+10$ days was taken as the systematic error.

Results Since the different spectral templates are often used together with various light-curve fitting techniques, the comparisons we report here are somewhat oversimplified.

Template differences using only epoch 0 values, mode (i), was found not to be dominating. But in mode (ii) serious systematic shifts do occur. The cosmological fits performed using the maximal difference between the templates, roughly differ by 2σ. While not being a totally realistic comparison, it shows the key importance of using accurate SN Ia templates. These plots are available through the webpage and the SMOCK Gui (see §6.3 below).

5.8. SN Ia brightness evolution

It is quite likely that the luminosity of the supernova is related to the properties of the white dwarf progenitor star, its companion and details of the propagation of the explosion. On the progenitor side, key parameters are the mass of the exploding white dwarf, the relative amounts of carbon and oxygen and metallicity. Thus, evolution in any of these parameters is a source of concern as it would lead to a drift in the intrinsic luminosity used to derive distances. In order to mimic an evolution of this kind, the effects of a redshift dependent bias were studied. This bias was described by a simple linear function of redshift, $\Delta M = kz$, where the slope k can be positive or negative.

Results Positive or negative evolution of intrinsic SN Ia brightness with redshift produce mainly bias effects. In general, an evolution of $|k| \sim 0.1$ is needed to cause significant bias. We show the effects of evolution in the (Ω_M, w)-plane in Figure 4, where a clear bias in both Ω_M and w can be seen (as expected, the relative area stays the same).

6. Discussion

Concerning our present knowledge of dark energy parameters, it is plausible that current data sets of SNe Ia are plagued by significant systematic uncertainties, such as cross-calibration errors, spectral template flaws, and uncertain extinction corrections. Systematic uncertainties may already dominate the error budget and will certainly do so in the future. To investigate, understand, and ultimately reduce or correct for these sources of error are hence of uttermost importance for the success of future precision cosmology.

The purpose of this paper is twofold: to present a method to investigate the impact on the estimation of cosmological parameters due to a number of systematic effects and, as an example, investigate the potential impact of systematic uncertainties in the cosmology fits of the Gold data-set of Riess *et al* 2007.

The SMOCK method, and all results for the Gold sample presented here, are somewhat dependent on the actual redshift binning used for the investigation and the details of the data set. Future improvements would include some form of parameterization of these effects as well.

In general, any future reported deviation from a ΛCDM-cosmology would need to be supplemented with excellent control of all systematics discussed here, since most of them could account for such a result.

6.1. Nightmare scenarios

Various "nightmare" scenarios can easily be constructed out of the systematic effects considered here. Miscalibration between low and high-z data and biased colors would lead to large systematic effects.

For example, any individual application of either an offset in inrinsic colors $\Delta(B-V) \sim 0.02$, a linear evolution of the lightcurve shape-brightness corrected peak brightness of SNe Ia exceeding $\Delta M = 0.1 \cdot z$ or a mean value of R_V of 2, instead of 3.1, would be enough to breach the statistical limit for the Gold data set.

Should any of these effects be combined or added to template uncertainties, systematic effects several times current statistical errrors *could* be generated.

6.2. DETF

Comparing any results presented here with the targets set by the Dark Energy Task Force (DETF)[33] for future ("stage four") instrument targets, it is clear that statistical errors will decrease significantly (as $1/\sqrt{n}$ where n is the number of SNe Ia). But systematic effects will not scale in the same way, meaning that the points of systematic-statistic equality for *bias* studies also will scale as $1/\sqrt{n}$. Future surveys will thus be *extremely* sensitive to systematic effects, and *any* bias will most likely come to dominate over statistical errors.

Thus, to make use of data from fourth generation instruments, control over instrumentation and calibration issues must be excellent. At the same time we can hope for a significant increase in the knowledge of understanding of systematic effects of astrophysical origin (developments are not easy to predict and are often not included in instrumentation plans but might be essential for future surveys).

6.3. SMOCK GUI

In order to help visualize the effects on the estimation of cosmological parameters due to systematic uncertainties, we have developed a small graphical application. This Graphical User Interface (GUI) displays the results obtained by the simulations performed with SMOCK. The application combines all results obtained for a particular data-set and allows different combinations of errors to be tried out. This tool, together with some of the data obtained for the Gold data-set, is available at www.physto.se/˜nordin/smock.

It should be noticed that all errors were calculated *individually*. In particular, a combined error in redshift and color-determination often leads to larger errors (e.g. through increased K-correction errors) than those displayed by the GUI.

7. Conclusions

SMOCK, a statistical Monte Carlo simulation approach towards quantification of systematic effects is presented. This method can give concrete answers to how sensitive SN Ia samples are to a wide variety of different systematic effects. We can estimate *both* systematic and statistical uncertainties in a time efficient way.

Current SN Ia data-sets are likely to be influenced by unknown systematics, which quite possibly already are larger than the statistical errors. In order for future SN Ia surveys to be successful, the propagated effects into the cosmolgical fits must be understood. With the methods presented here this will be possible through a process where we first define acceptable systematic uncertainties to achieve some target confidence level in e.g. the impact on the derived dark energy properties. The SMOCK technique can be used to further define the instrumental requirements necessary to detect and possibly correct for any putative source of systematic uncertainty.

Studies of a range of different systematics were performed on the Gold data-set, demonstrating the possibility of quantifying sensitivity to systematic effects. The importance of excluding the effects of a possible R_V or color bias and obtaining a good spectral template were highlighted. For increased precision future surveys will need to demonstrate that maximal systematic color effects are at the 0.01 magnitude level and that host galaxy dust properties do not have any systematic shifts over the $\Delta R_V = 1$ level (or that possible such shifts are under control).

Acknowledgments

AG would like to acknowledge support by the Swedish Research Council and the Göran Gustafsson Foundation for Research in Natural Sciences and Medicine.

[1] Goobar A and Perlmutter S, 1995 *Astrophys. J.* **450** 14
[2] Garnavich P *et al* , 1998 *Astrophys. J.* **509** 74
[3] Riess A *et al* , 1998 *Astron. J.* **116** 1009
[4] Schmidt B P, *et al* 1998 *Astrophys. J.* **507** 46
[5] Perlmutter S *et al* , 1999 *Astrophys. J.* **517** 565
[6] Knop R A *et al* , 2003 *Astrophys. J.* **598** 102
[7] Tonry J *et al* 2003, *Astrophys. J.* **594** 1
[8] Barris B *et al* , 2004 *Astrophys. J.* **602** 571
[9] Riess A *et al* , 2004 *Astrophys. J.* **607** 665
[10] Astier P *et al* , 2006 *Astron. Astrophys.* **447** 31
[11] Wood-Vasey W M *et al* , 2007, *preprint* astro-ph/0701041
[12] Riess A *et al* , 2007 *Astrophys. J.* **659** 98
[13] Neill J D, Hudson M J and Conley A, 2007 *preprint* arXiv:0704.1654
[14] Kim A, Goobar A, and Perlmutter S, 1996 *PASP* **108** 190
[15] Eisenstein D J *et al* , 2005 *Astrophys. J.* **633** 560
[16] Press W H, Teukolsky S A, Vetterling W T, and Flannery B P, 1992 *Numerical Recipies in FORTRAN. The Art of Scientific Computing* (Cambridge:University Press, 2nd ed.) p 406
[17] Goobar A *et al* , 2002, *Astron. Astrophys.* **392** 757
[18] Hamuy M, Phillips M M, Suntzeff, N B, *et al* , 1996 *Astron. J.* **112** 2438
[19] Riess A G, KirshnerR P, Schmidt B P, Jha S, *et al* . 1999 *Astron. J.* **117** 707
[20] Jha S *et al* , 2006 *Astron. J.* **131** 527
[21] Fitzpatrick E, 1999 *PASP* **111** 63
[22] Perlmutter S *et al* , 1997 *Astrophys. J.* **483** 565
[23] Mobasher B *et al* , 2004 *Astrophys. J.* **600** L167
[24] Ilbert O *et al* , 2006 *Astron. Astrophys.* **457** 841
[25] Mobasher B *et al* , 2007 *Astrophys. J. Supp.* **172** 117
[26] Jönsson J *et al* , 2006 *Astrophys. J.* **639** 991
[27] Nugent P, Kim A, and Perlmutter S, 2002 *PASP* **114** 803
[28] Nobili S *et al* , 2003 *Astron. Astrophys.* **404** 901
[29] Guy J *et al* , 2005 *Astron. Astrophys* **443** 781
[30] Guy J *et al* , 2007 *preprint* astro-ph/0701828
[31] Hsiao E *et al* , 2007 *preprint* astro-ph/0703529
[32] Podsiadlowski P *et al* , 2006 *preprint* astro-ph/0608324
[33] Albrecht A *et al* , 2006 *preprint* astro-ph/0609591